Science AAAS

www.sciencemag.org/content/343/6175/1248765/suppl/DC1

Supplementary Materials for

Dynamic Reorganization of River Basins

Sean D. Willett,* Scott W. McCoy, J. Taylor Perron, Liran Goren, Chia-Yu Chen

*Corresponding author. E-mail: swillett@erdw.ethz.ch

Published 7 March 2014, *Science* **343**, 1248765 (2014)
DOI: 10.1126/science.1248765

The PDF file includes:

Figs. S1 to S15
Tables S1 and S2
Caption for movie S1

Other supplementary material for this manuscript includes the following:

Movie s1
Databases S1 to S9

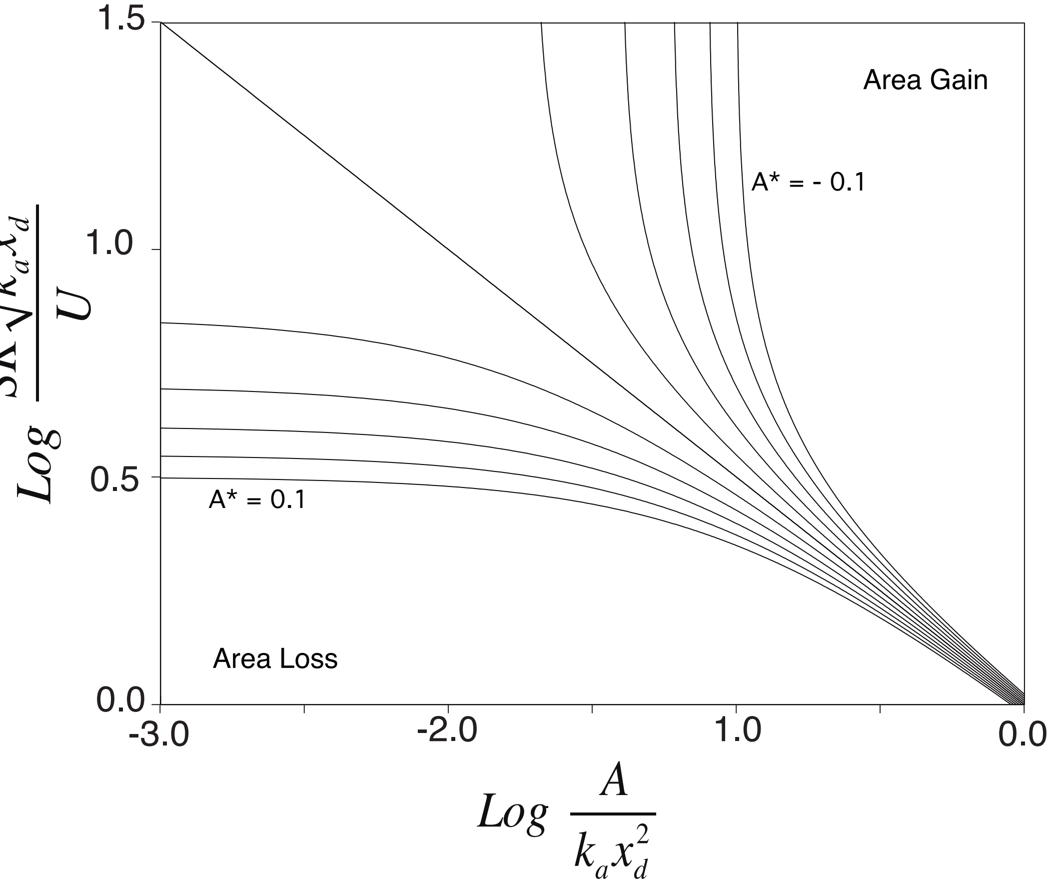

Fig. S1. Disequilibrium effect of changing area on slope-area plot. Slope, Area relationship for a basin experiencing an instantaneous change in drainage area at its headwater. *A** is a fractional change to the initial basin area and varies from negative 10% to positive 10% with an increment of 0.02. Slope, *S* and drainage area, *A* are non-dimensionalized by the channel steepness and the initial area of the basin. Area changes of a few percent will induce large deviations from the expected linear trend on a log-log plot.

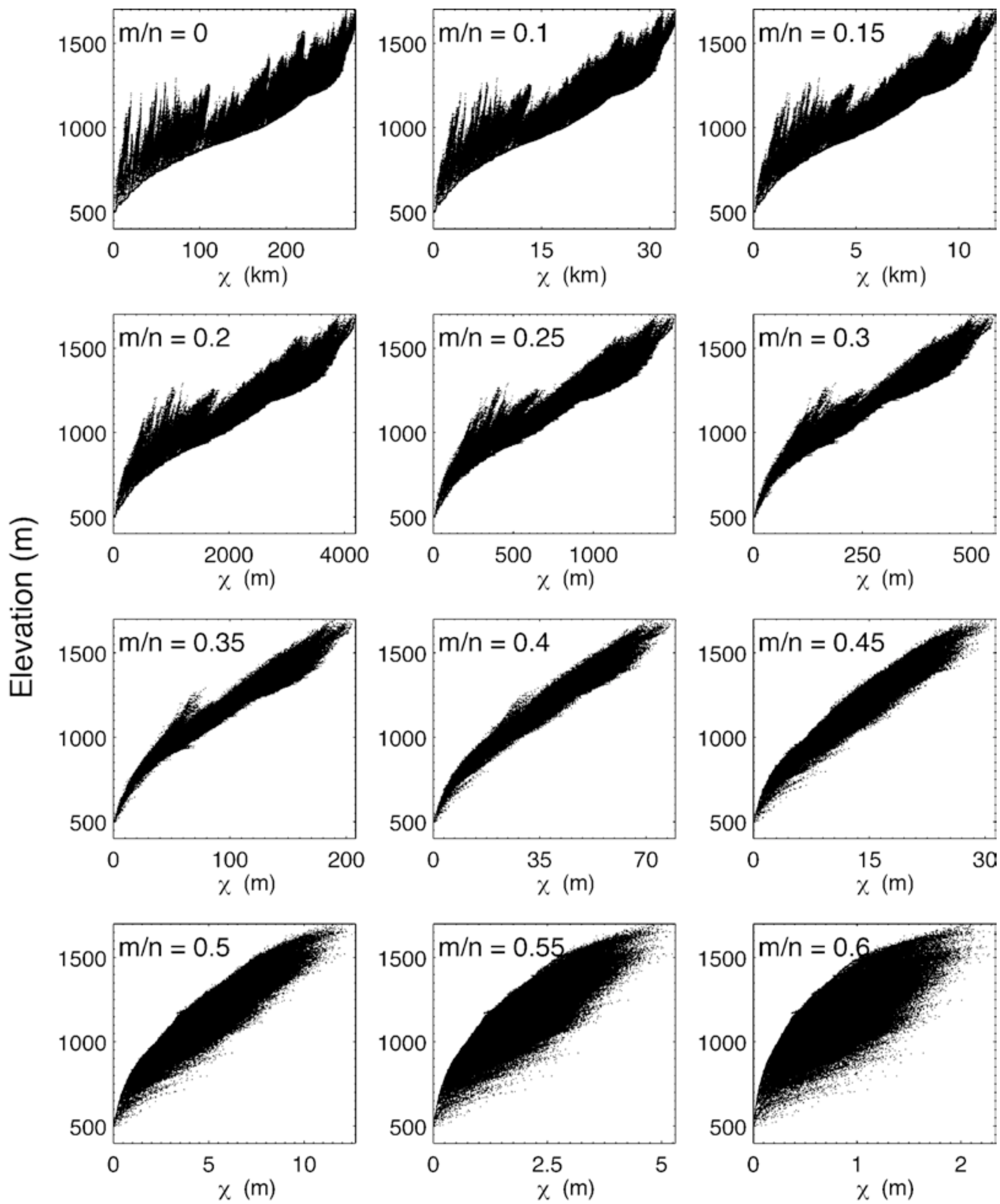

Fig. S2: χ -plot for the Yanhe and Qingjian tributaries of the Yellow River, China.

Plots are constructed using a range of concavity from 0 to 0.6. A concavity of 0.0 reduces χ to river distance from base level, so the upper left shows the longitudinal profiles of the rivers. In the case of the Yellow River, we expect the drainages to be near equilibrium, so we select the concavity that best minimizes scatter in the plot, which is 0.35. Note that the concavity value that best reduces scatter does not produce a linear χ plot, but rather a convex-up profile. This suggests that the entire Yellow River basin is experiencing an increase in incision rate. Interestingly, analysis of the χ map for this region shows that this change is not inducing significant topological reorganization. The stationarity of divides, despite an increase in incision rate, suggests that the landscape had reached a steady state before the increase in incision rate.

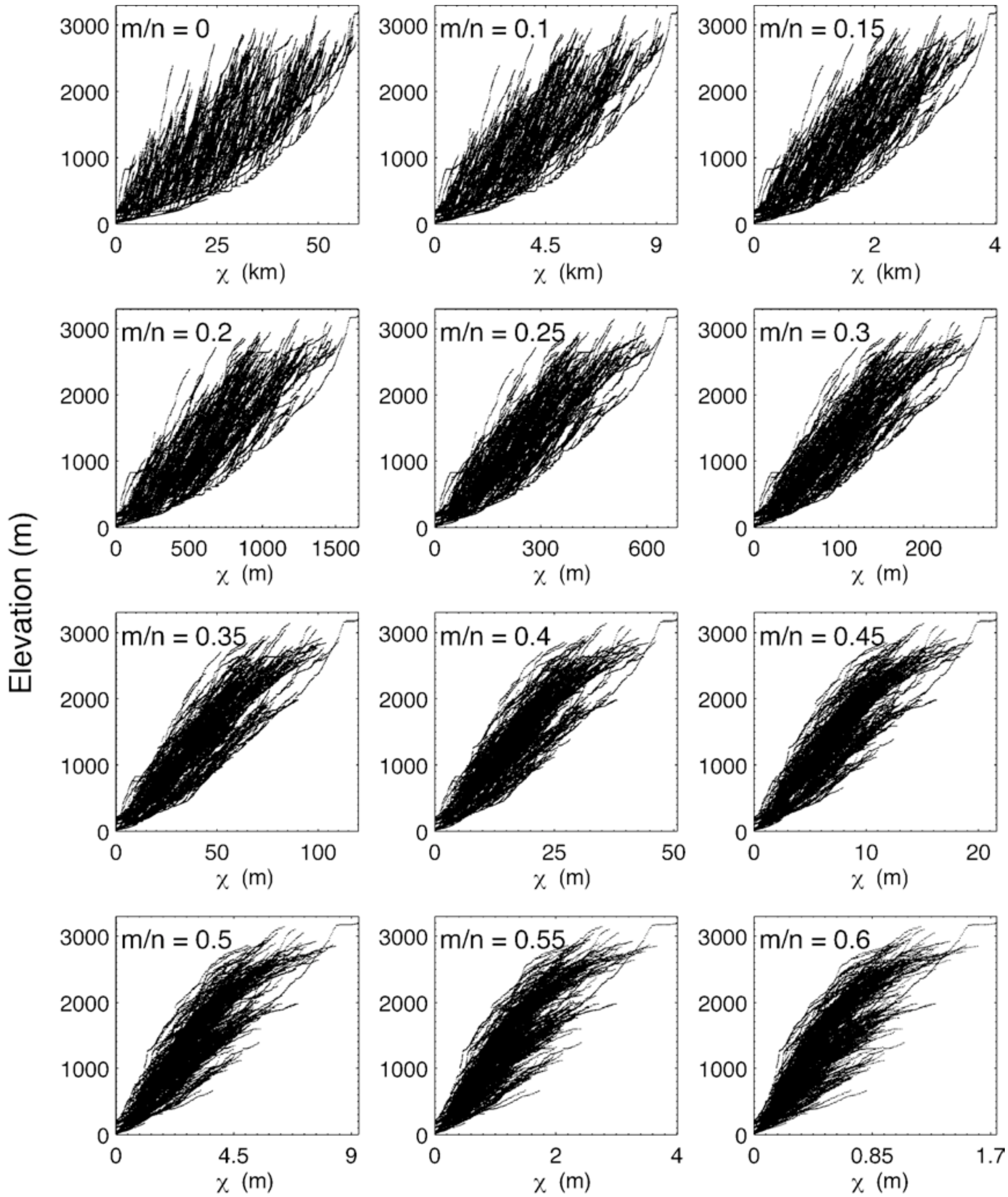

Fig. S3: χ -plot for the Eastern Central Range of Taiwan.

Plots are constructed using a range of concavity from 0 (river profiles) to 0.6. Given the youthful landscape, we expect considerable disequilibrium and changing area, and the large scatter in the χ plots supports this interpretation. The minimum scatter is obtained for a concavity of 0.3 to 0.4, but we favor a slightly higher value. In a system with many moving divides and captures, we expect to have many channels with low χ plot slopes and high χ and also many channels with kinks in the χ plot in response to capture. These features become more obvious with concavities of 0.45 to 0.55, so we prefer this value and use a value of 0.5 for the maps of χ .

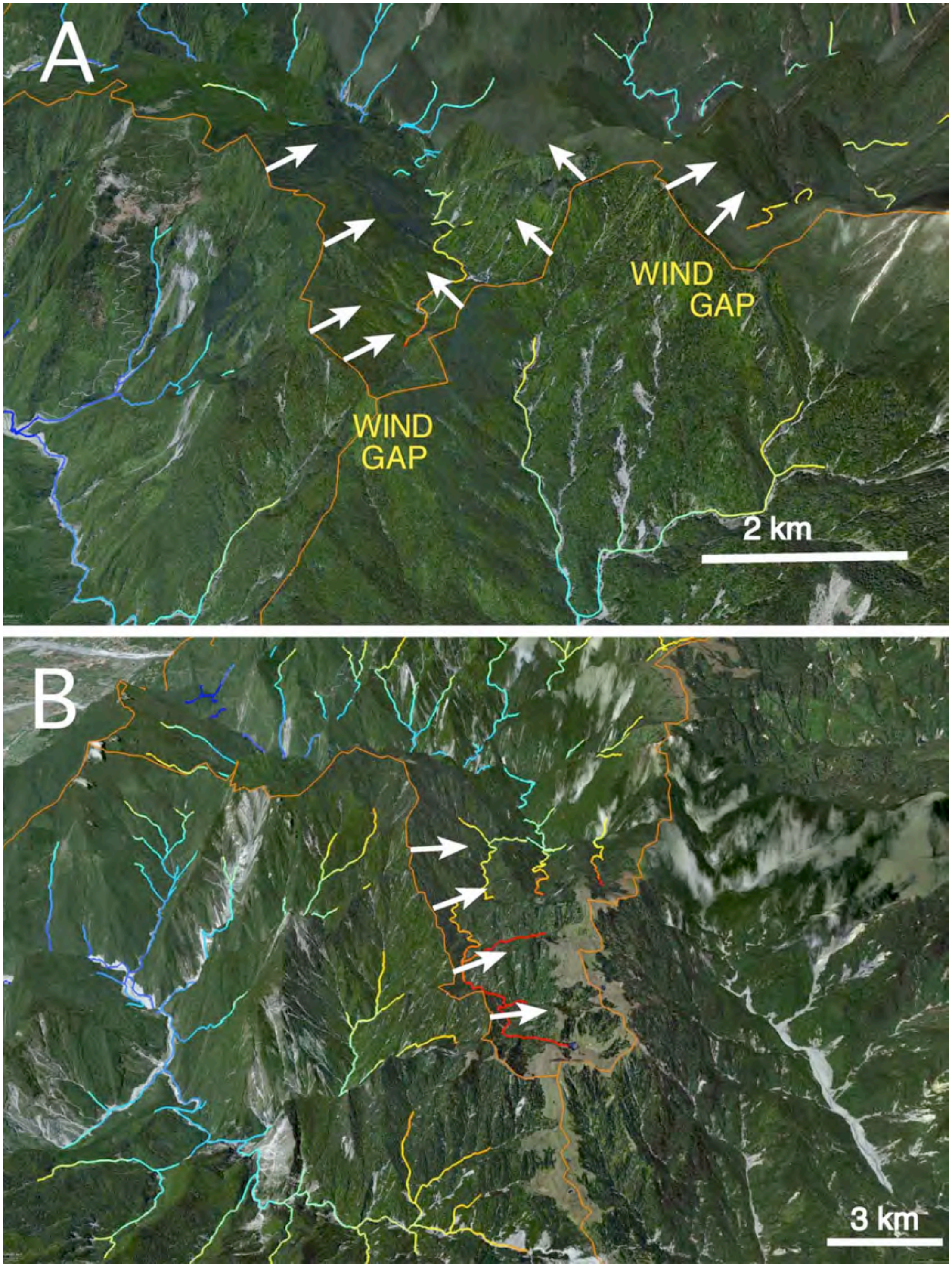

Fig. S4. Map of χ draped over topography and satellite imagery of a region of eastern Central Range, Taiwan. View location indicated in Figure 5. Vertical exaggeration is 2x. A: Migration of divide from low χ to high χ channel has left asymmetric divide with nearly complete truncation of some channel heads leaving wind gaps. B: Divide migration from low to high χ has pushed divides to near high χ, "perched" tributary. Capture is imminent. Images are constructed using Google Earth.

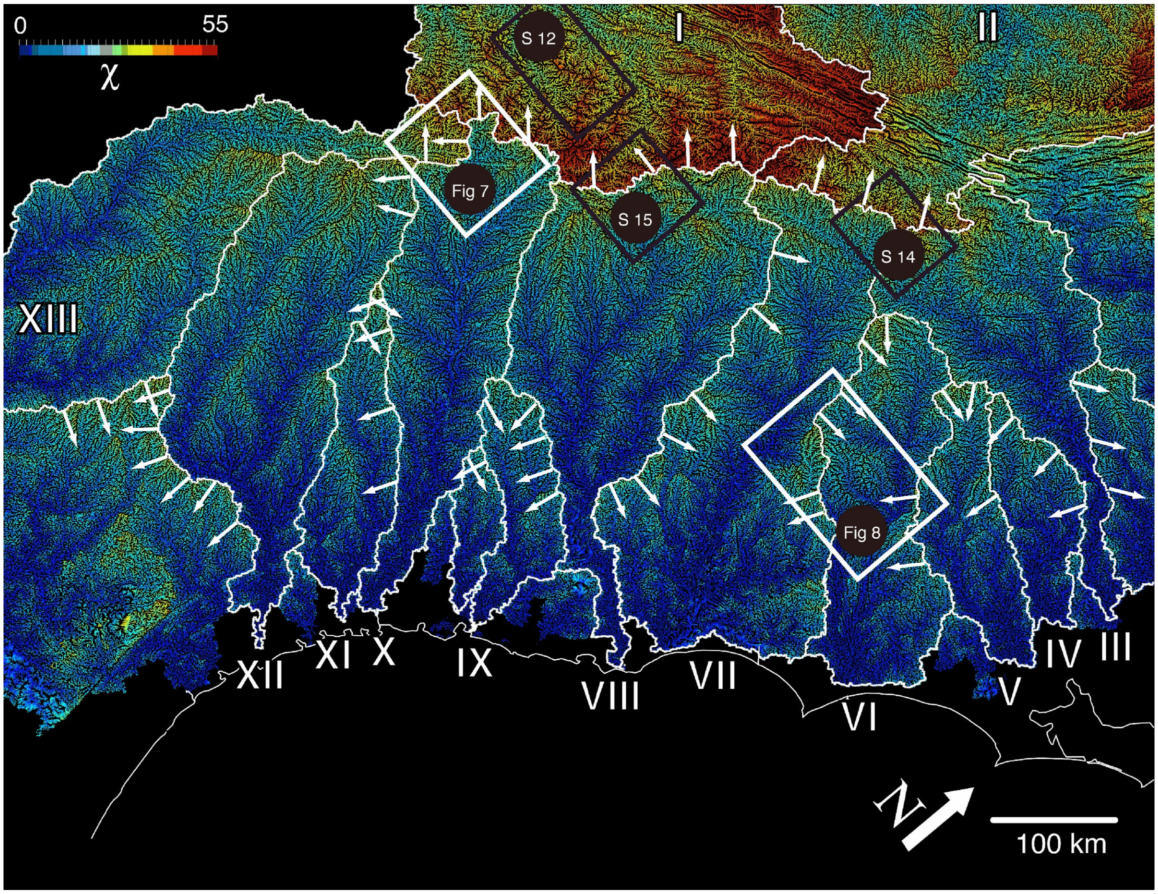

Fig. S5. Map of χ for the southeast USA using a concavity of 0.45. White arrows indicate the migration direction of primary water divides inferred from discontinuity in χ across these divides. White boxes show locations of figures presented in the main text in which independent geological evidence from stream capture and highly asymmetric topography support inferred divide motion. Black boxes show locations of figures presented below that detail differential erosion rates estimated from cosmogenic radionuclide concentrations. Roman numerals correspond to the major drainage basins: I-Tennessee, II-Kanawha, III-Roanoke, IV-Pamlico, V-Neuse VI-Cape Fear, VII-Pee Dee, VIII-Santee, IX-Edisto, X-Savannah, XI-Ogeechee, XII-Altamaha, XIII-Apalachicola.

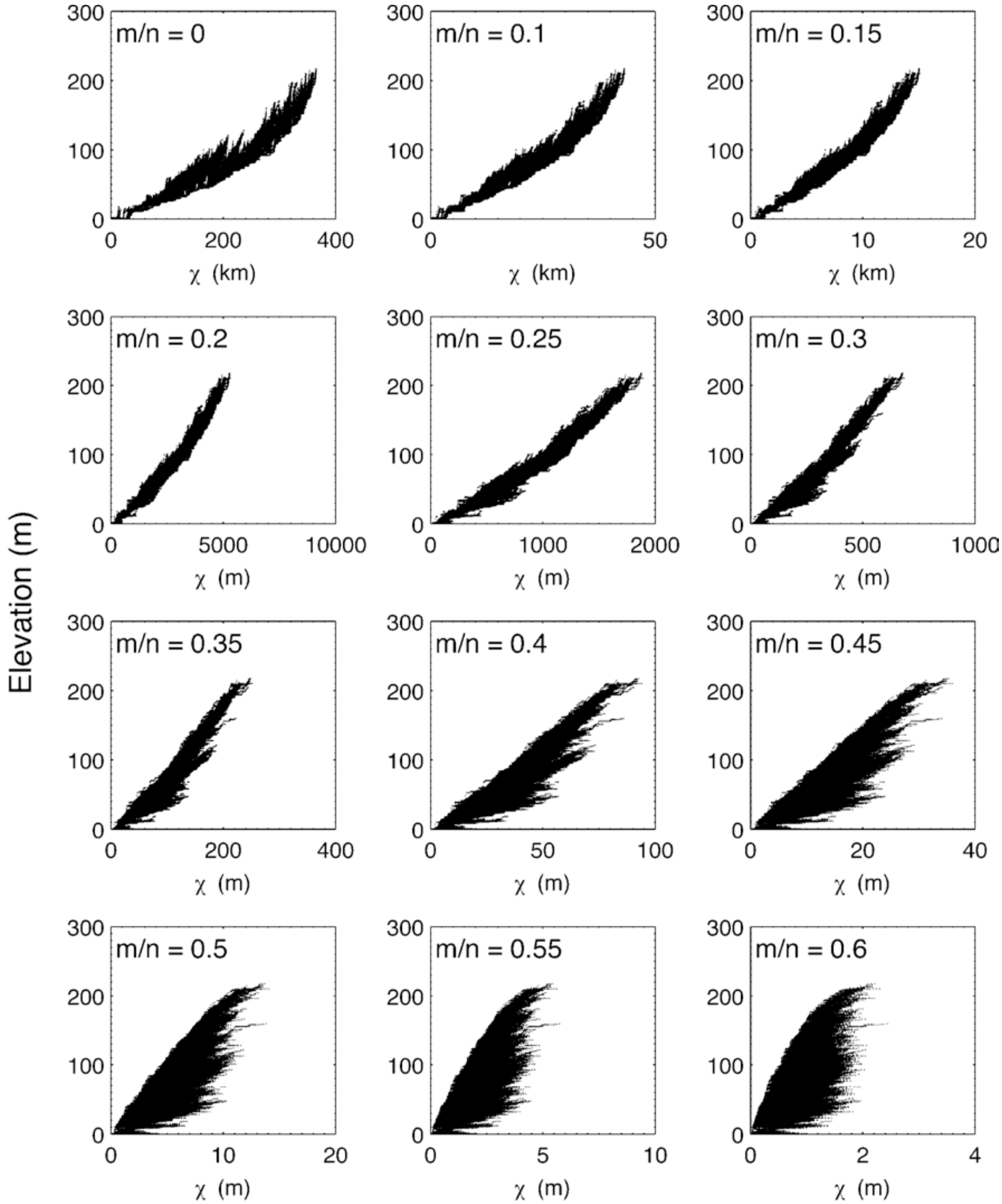

Fig. S6: χ-plots for the Ogeeche River, SE USA, for a range of m/n **values.** See Figure S5 for location. Based on a combination of independent lines of evidence such as geologic evidence of discrete stream capture, topographic asymmetry of divides, or differential erosion rates across divides inferred from measurements of the concentration of the cosmogenic radionuclides (see section below) basins were interpreted as dominantly gaining or losing area. Using this methodology, the Ogeeche Basin is interpreted as losing area. A basin that is dominantly losing area around its perimeter should exhibit convex-up χ plots. Convex-up profiles are observed with m/n values greater than 0.4.

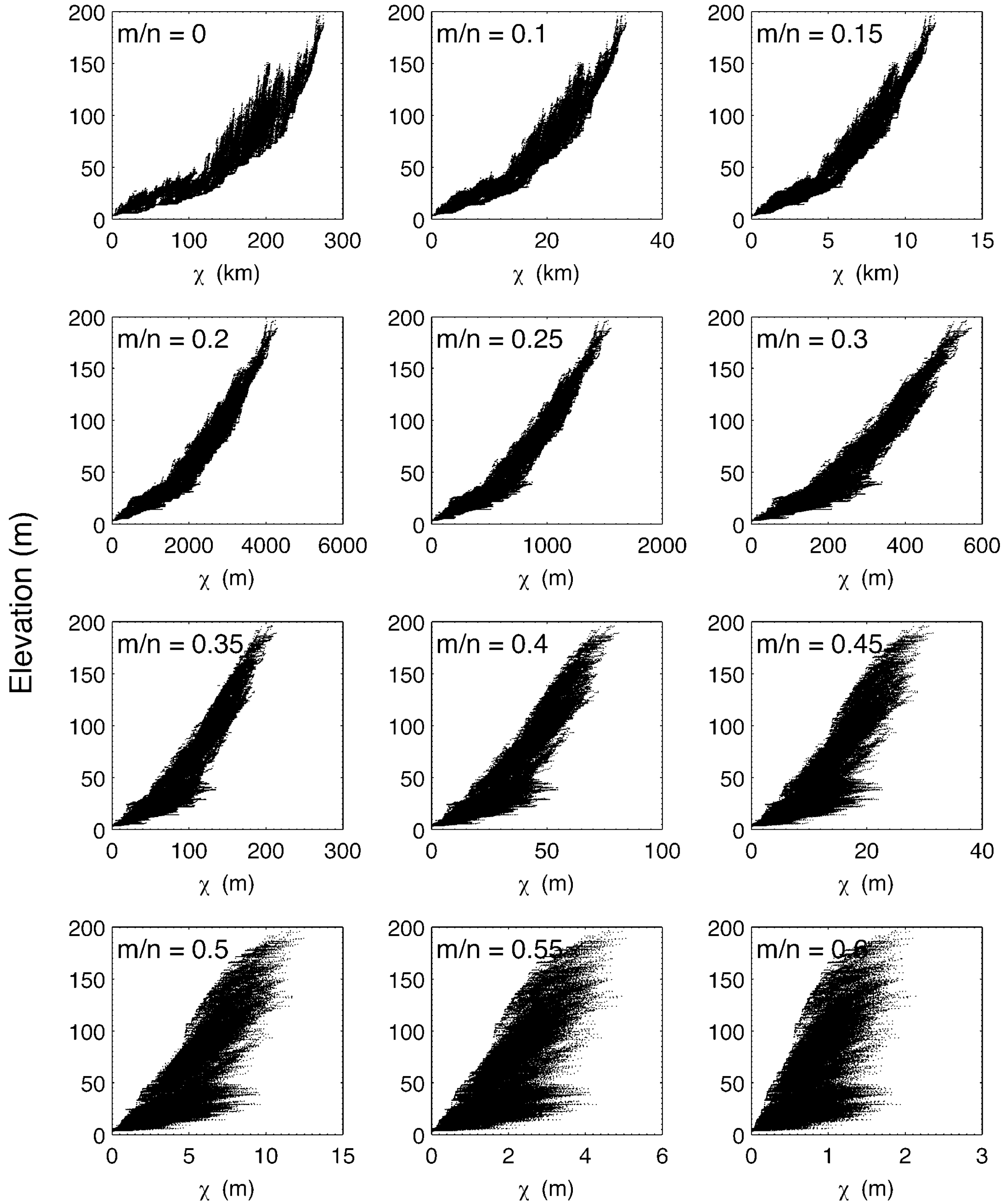

Fig. S7: χ - plot for the Pamlico River, SE USA, for a range of m/n **values.** See Figure S5 for location. For reasoning given in Figure S6, basin is interpreted as losing area, so preferred m/n is greater than 0.4.

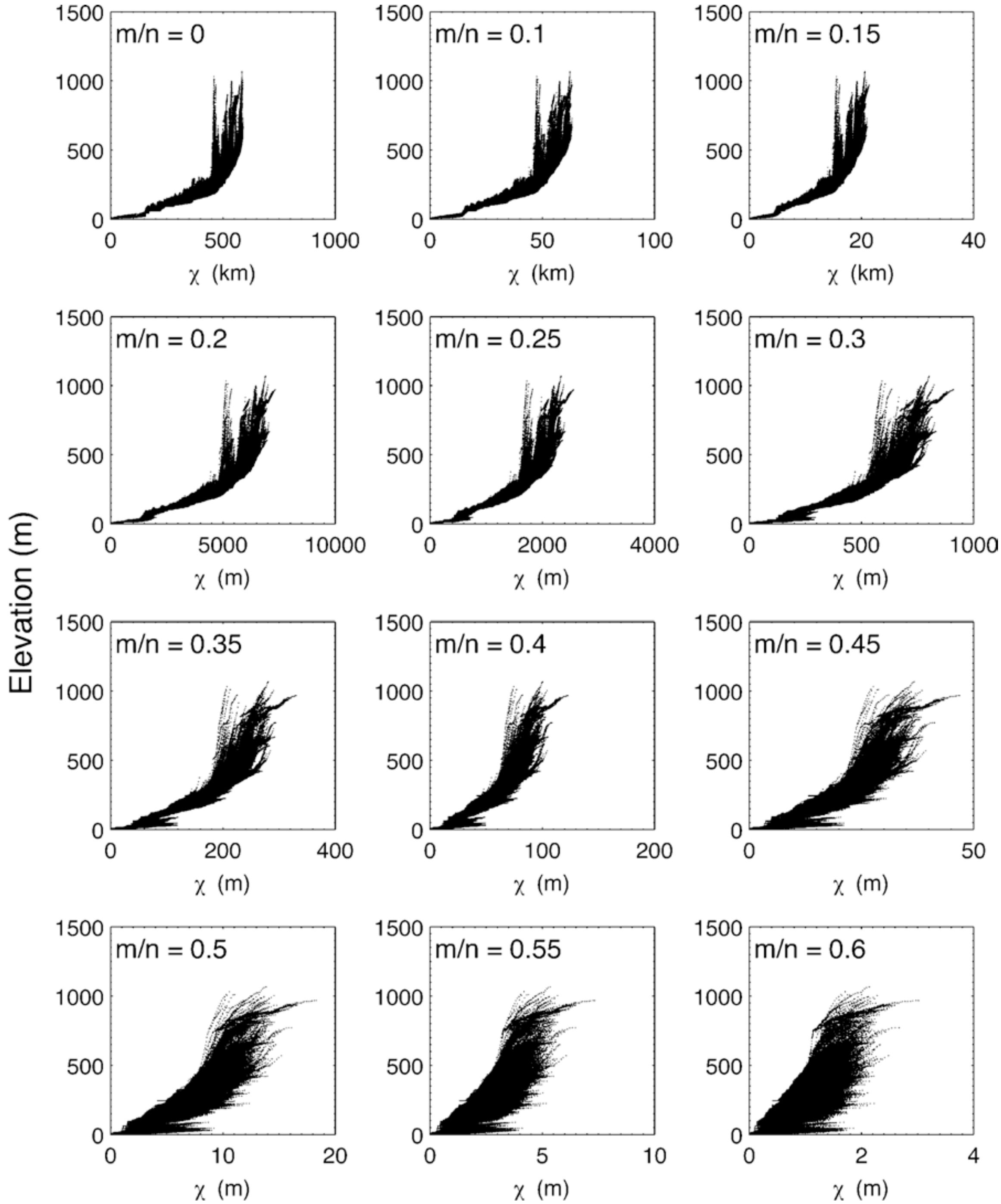

Fig. S8: χ -plot for the Roanoke River, SE USA for a range of m/n values. See Figure S5 for location. The Roanoke is growing to the west by retreat of the Blue Ridge escarpment. Area gain is, in part, achieved though discrete river capture, so in addition to the predominately concave up χ plots, we expect some tributaries to exhibit the capture-related pattern seen in Figure 2 with a steep segment leading to a lower-steepness captured reach. Predominately concave up χ plots and clear capture signatures are evident for m/n values greater than 0.4 and less than about 0.55.

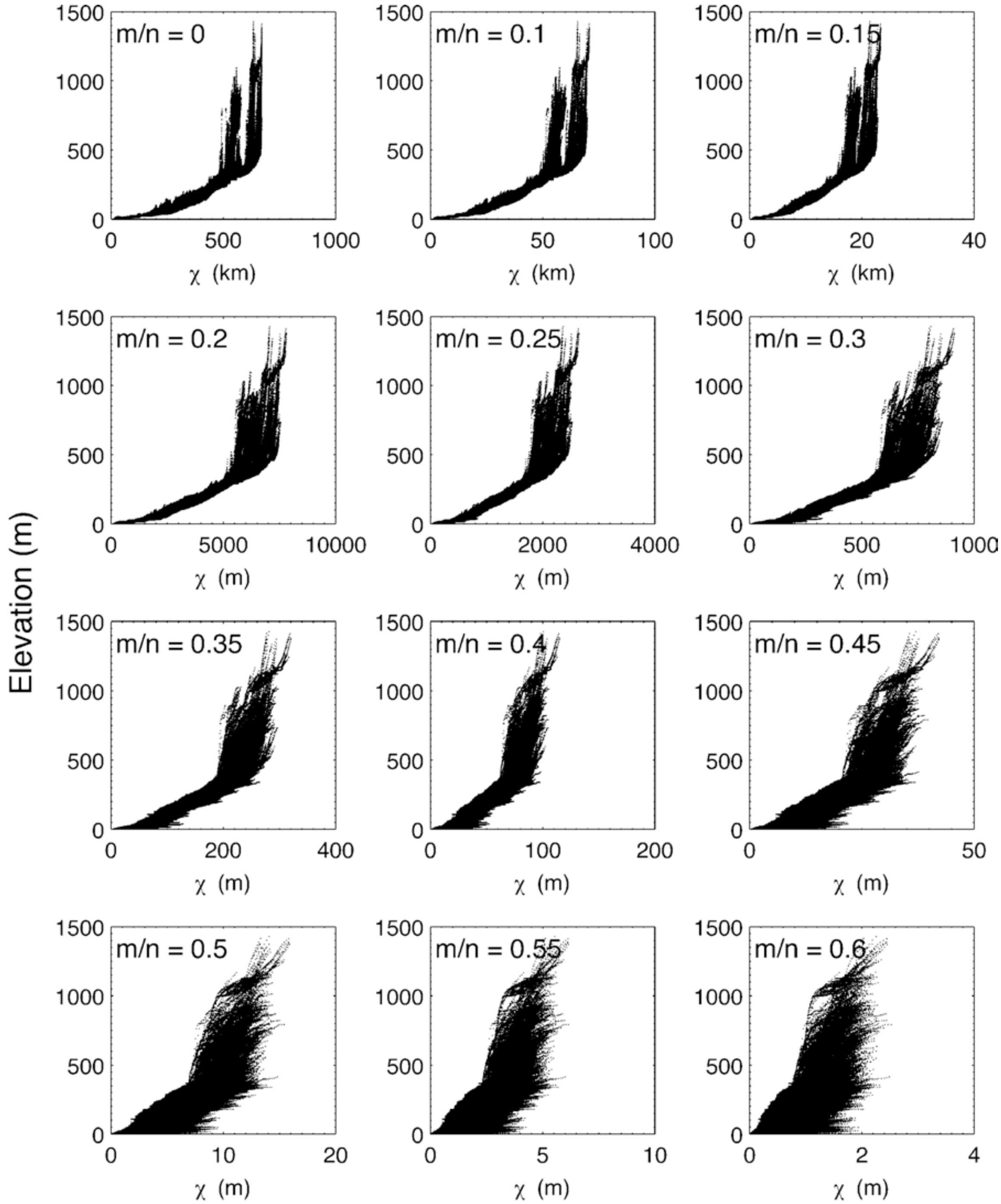

Fig. S9: χ -plot for the Santee River, SE USA, for a range of m/n values. See Figure S5 for location. For reasoning given in Figure S6, basin is interpreted to be dominantly gaining area by divide migration and river capture, so preferred m/n is greater than 0.4, but less than 0.55.

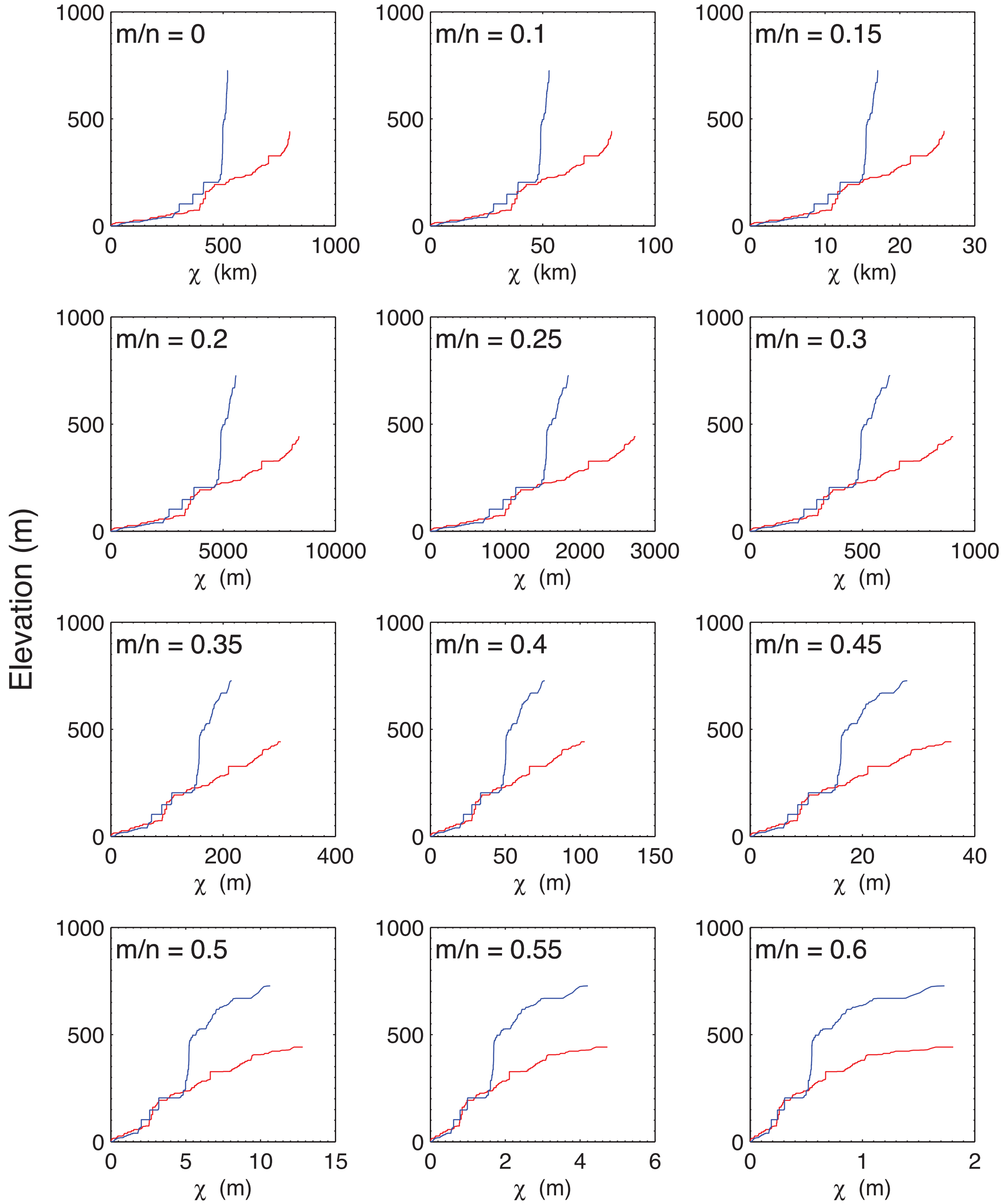

Fig. S10: χ -plots for tributaries of the Savannah River and the Apalachicola River. See main text and Figures 6 and 7 for location. The Savannah (blue) is interpreted as having captured the headwaters of the Apalachicola (red), so we expect characteristic shapes to the χ-plots (Figure 2), which can be used to calibrate concavity. The expectation is that the river losing area (Appalachicola) will be convex up. This is most clearly true for concavities larger than 0.45. Similarly, the upper captured reach of the Savannah is expected to have a slope similar to the present Apalachicola, which is observed only for concavity larger than 0.45.

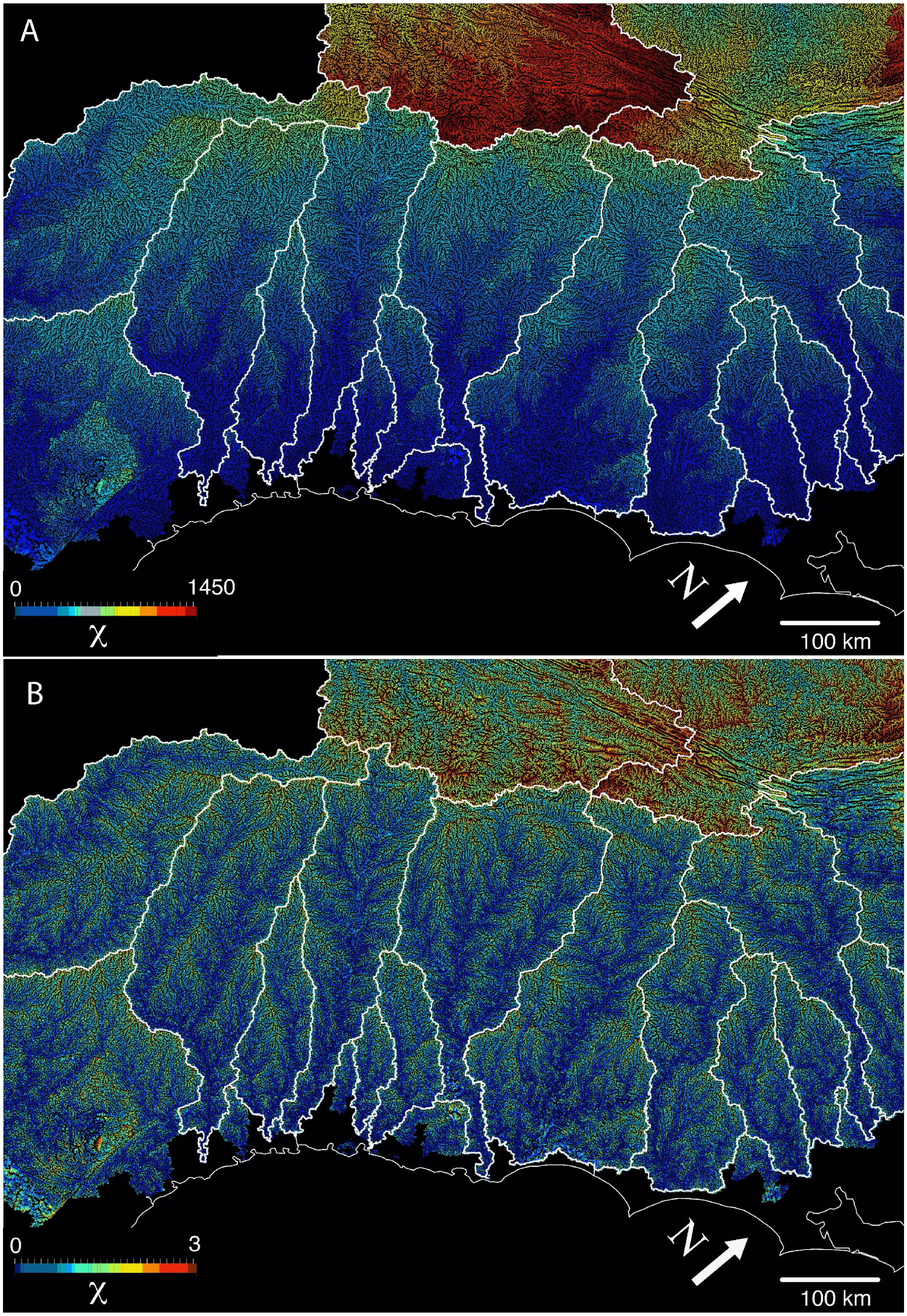

Fig. S11: Maps of χ for the southeast USA for a range of m/n values. Maps were constructed using a concavity of (A) 0.3 and (B) 0.6. Compare with Fig. 6. Although there are significant changes between maps, the relative values of χ across water divides rarely change. The major features such as the escarpment or the features discussed in Figures 7 and 8 remain.

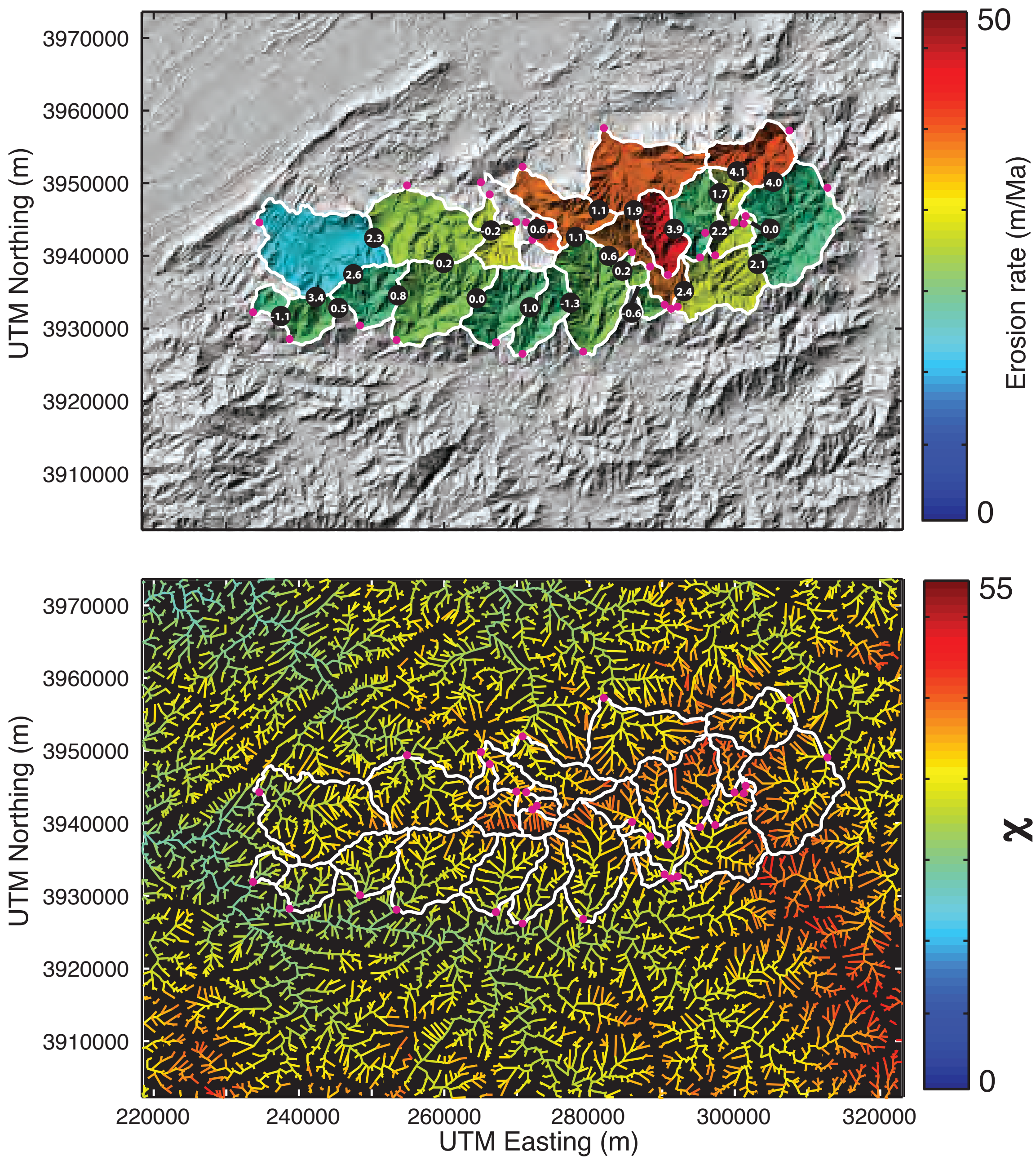

Fig. S12: Erosion rate and χ maps of the Great Smoky Mountains, Southeast USA. Upper map shows shaded relief map with basin-averaged erosion rates indicated by colors draped over each sampled basin. Erosion rates compiled by Portenga and Bierman (*10*). Basin mouths marked by magenta circles. Numbers within black circles are the negative mean difference of channel head χ values (lower figure) along the divide segment. The erosion rate difference across each divide segment marked with a black circle is plotted against its respective $-\Delta\chi$ value in the inset of Figure 6. χ is calculated using a concavity of 0.45. Maps projected in UTM zone 17.

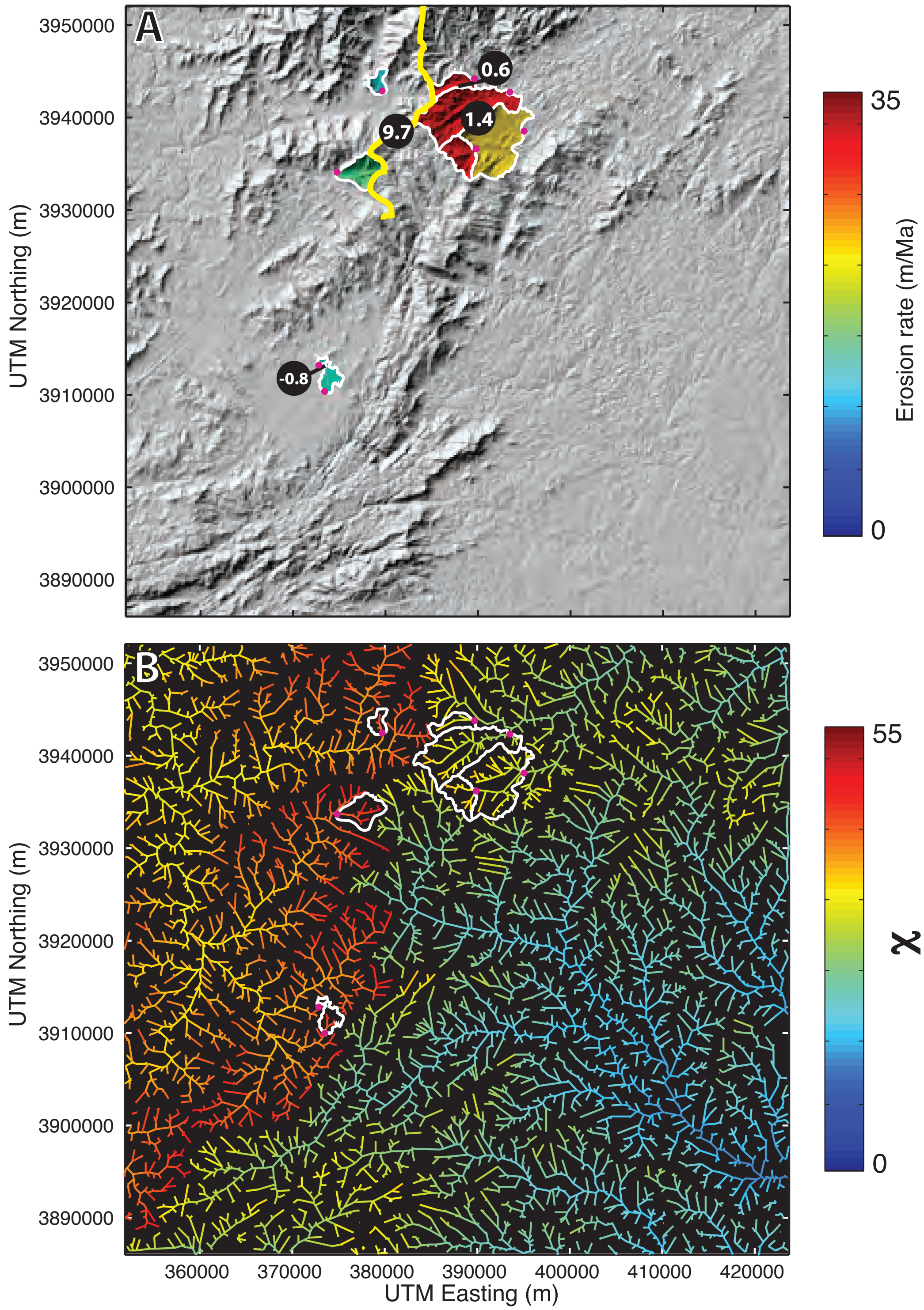

Fig. S13: Erosion rate and χ maps of a southern segment of the Blue Ridge Escarpment, Southeast USA. A: Same as that described in Figure S12, with the exception that $-\Delta\chi$ value reported in a black circle above a thick yellow line is the negative mean difference of channel head χ values along the portion of the escarpment demarcated by the yellow line. B: χ map as described in Figure S12. Maps projected in UTM zone 17.

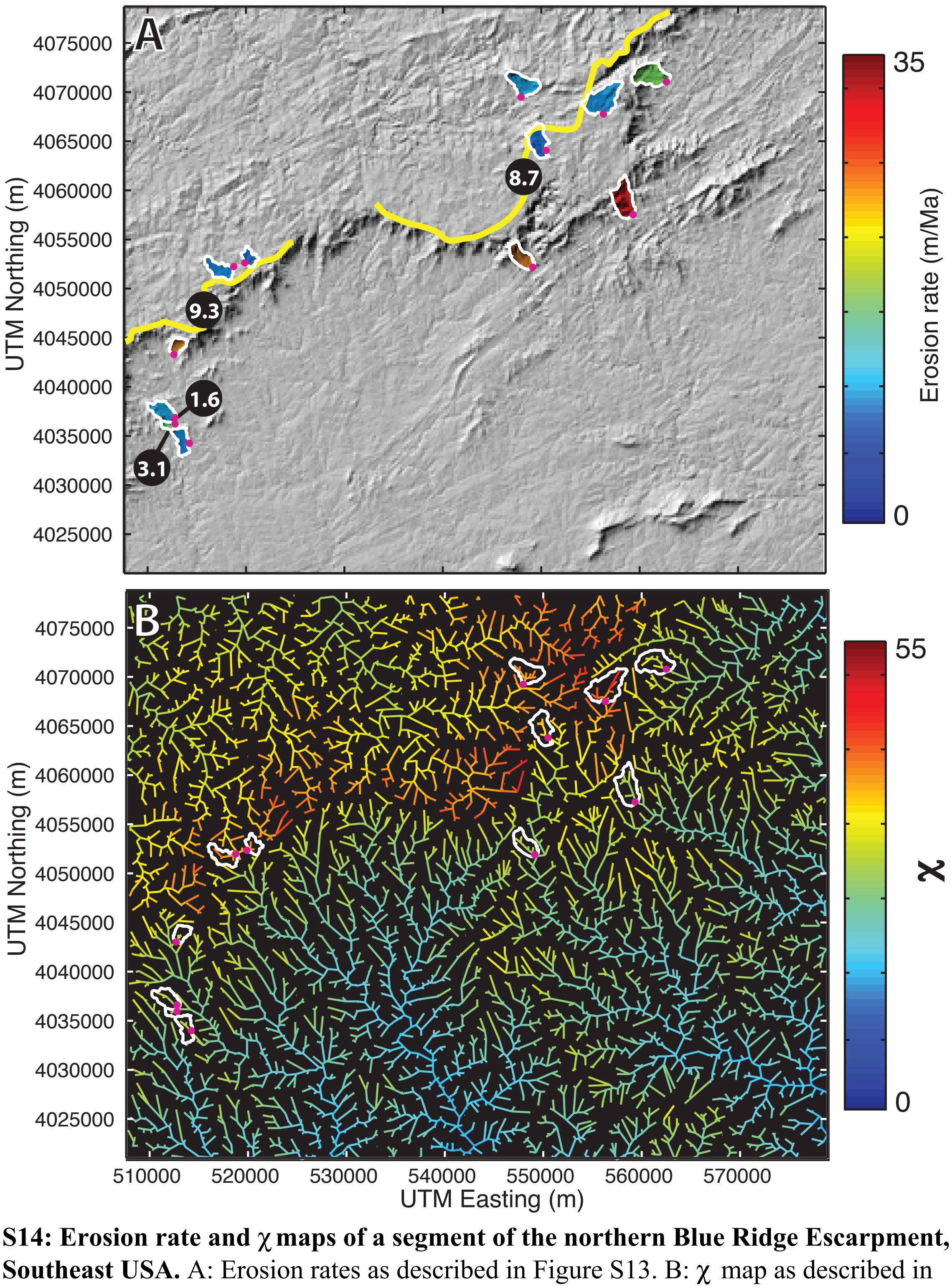

S14: Erosion rate and χ maps of a segment of the northern Blue Ridge Escarpment, Southeast USA. A: Erosion rates as described in Figure S13. B: χ map as described in Figure S13. Maps projected in UTM zone 17.

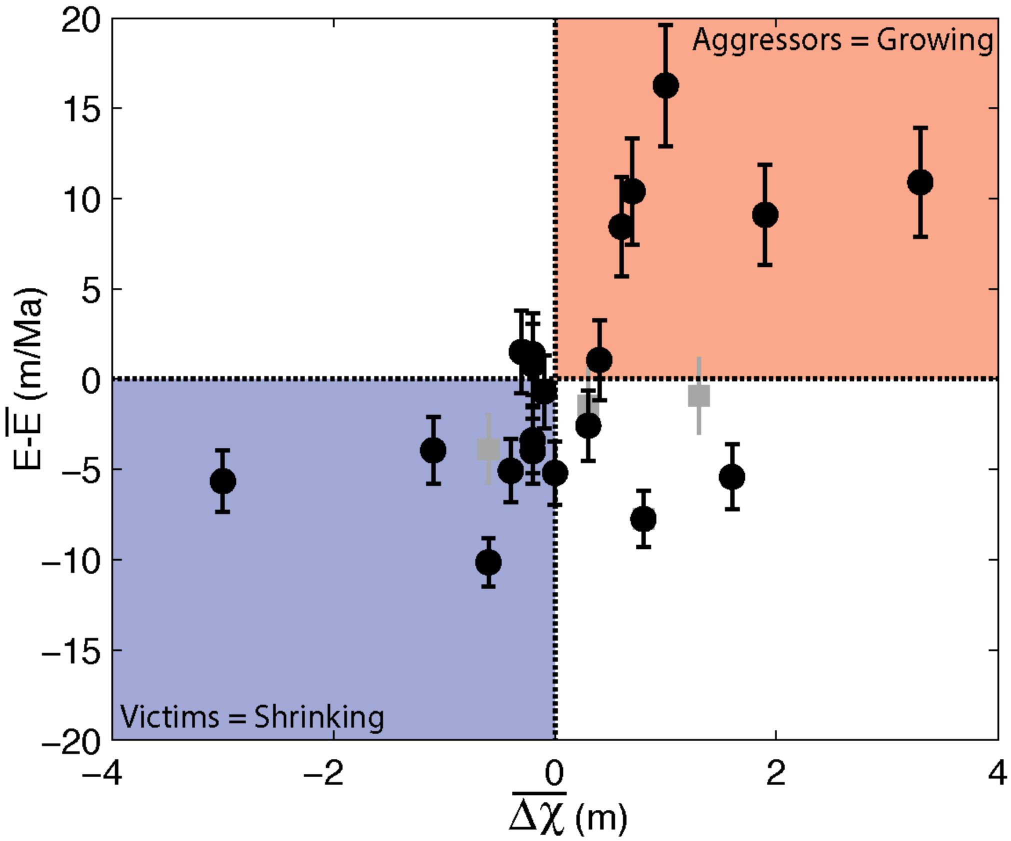

S15: The relationship between cross divide χ and erosion rate in the Great Smoky Mountains, Southeast USA. The deviation of local basin-averaged $(E - \bar{E})$ erosion rate from the regional mean is plotted as a function of the mean difference of channel head χ values around the entire perimeter of the basin ($\overline{\Delta\chi}$). $\overline{\Delta\chi}$ can be considered a basin aggressivity metric, in which positive values indicate basins that are likely growing at the expense of their neighbors, whereas basins with negative values are victims expected to be shrinking. If area change, as characterized by χ, is the dominant influence on erosion rate, a basin is expected to plot in the upper right or lower left quadrant. We observe that 20 out of 23 analyzed basins lie in, or have uncertainties overlapping, the expected quadrant, showing that a significant fraction of the variance can be explained by changing area. Grey points are basins with an area less than 10 km^2.

Table S1.

Drainage basins characteristics used in the inset of Figure 6 and S12-S14. Cross-divide χ and erosion rates from ^{10}Be concentrations. Sample names correspond to those used by Portenga and Bierman (10).

Sample names from differenced basins	$\Delta\chi$ (m)	ΔE (m/Ma)	$\Delta\chi/\bar{\chi}$	$E/\bar{E}$
Great Smoky Mountains				
GSTM-1 - GSPB-1	1.10	1.42	0.036	0.063
GSTM-1 - GSEC-1	-0.50	1.20	-0.015	0.053
GSHC-1 - GSEC-1	-0.80	2.62	-0.023	0.112
GSHC-1 - GSFC-1	0.00	1.87	0.000	0.079
GSFC-1 - GSNC-1	-1.00	0.30	-0.029	0.013
GSDC-1 - GSNC-1	1.30	2.81	0.037	0.117
GSCO-2 - GSDC-1	-0.60	10.38	-0.016	0.340
GSCO-4 - GSRF-11	-3.90	21.92	-0.097	0.673
GSCO-2 - GSRF-12	-2.35	6.94	-0.061	0.215
GSRF-6 - GSRF-1	-1.70	5.32	-0.043	0.205
GSRF-10 - GSRF-11	-2.20	6.70	-0.055	0.268
GSRF-12 - GSCA-1	-2.05	6.58	-0.050	0.258
GSLP-1 - GSWP-1	-1.10	1.30	-0.028	0.035
GSMP-1 - GSAC-1	-2.30	9.45	-0.064	0.433
GSTM-1 - GSAC-1	-3.40	6.15	-0.100	0.305
GSEC-1 - GSAC-1	-2.60	4.95	-0.072	0.253
GSMP-1 - GSHC-1	-0.20	1.88	-0.005	0.073
GSWP-1 - GSDC-1	-1.10	11.03	-0.028	0.358
GSLP-1 - GSCO-2	-1.90	1.95	-0.048	0.053
GSBC-2 - GSRF-10	-4.10	9.86	-0.103	0.297
GSBC-2 - GSCA-1	-4.00	15.98	-0.104	0.529
GSLR-5 - GSLR-6	0.20	1.61	0.005	0.056
GSCO-5 - GSCO-3	0.60	1.94	0.016	0.078
GSCO-5 - GSCO-6	-0.20	2.42	-0.005	0.098
GSRF-2 - GSRF-3	0.02	6.82	0.001	0.297
GSLR-4 - GSLR-2	-0.60	1.34	-0.015	0.034
Blue Ridge Escarpment				
CS-10 - CS-9	0.80	1.85	0.024	0.126
CS-19 - CS-20	-0.60	4.21	-0.019	0.136
CS-20 - CS-21	-1.40	6.24	-0.041	0.243
CS-04 - CS-05	-1.60	6.10	-0.057	0.458
CS-04 - CS-02	-3.10	6.93	-0.107	0.537
mean(CS-28,CS-31,CS-32) - mean(CS-27,CS-26,CS-25)	-8.70	16.00	-0.231	0.910
CS-6 - mean(CS-01,CS-08)	-9.34	15.61	-0.259	0.940
mean(CS-19,CS-20,CS-22) - mean(CS-18,CS-16)	-9.70	17.33	-0.243	0.771

Table S2.

Parameters used for χ maps presented in paper and provided in Data Archive. Summary of data files in Data Archive. Files are compressed kml format containing vector data of χ for rivers in each study area of main paper. Files can be viewed using Google Earth. Parameters for calculation are in table and include: θ, the concavity; A_c the critical or minimum area used to define channel network; A_0 the scaling area; χ_0, the minimum χ which is non-zero if the integration did not start at sealevel, and χ_M, the maximum value used to scale the color map.

File Name	Region	θ	A_c	A_0	χ_0	χ_M
Willett _Yanhe	Yanhe Basin	0.35	$.57 \times 10^4$	1	0	200
Willett _Qingjian	Qingjian Basin	0.35	$.57 \times 10^4$	1	0	200
Willett _Taiwan	Central Range, Taiwan	0.5	10^6	1	0	5.5
Willett _Virginia	Virginia	0.45	10^3	1	0	50
Willett _NC	North Carolina	0.45	10^3	1	0	50
Willett _SCGA	South Carolina, Georgia	0.45	10^3	1	0	50
Willett _Tennessee	Tennessee	0.45	10^3	1	8	50
Willett _UpperOhio	Upper Ohio	0.45	10^3	1	10	50
Willett _Cumberland	Cumberland	0.45	10^3	1	8	50

Movie S1. Numerical simulation showing the evolution of χ during landscape reorganization. The simulation uses the DAC landscape evolution model described in (*21*). The initial condition for the simulation is an asymmetrical mountain range that is in a steady state with respect to a linear gradient in the tectonic rock uplift rate that varies from 0.5 mm year^{-1} at the lower boundary to 5 mm year^{-1} at the upper boundary. The rock uplift rate is then set to a uniform value of 1 mm year^{-1}, and the landscape evolves to a new steady state through changes in river network topology, drainage basin geometry, and channel elevations. Divide migration at multiple scales is generally in the direction of the channel with higher χ. Topologic and topographic steady state are achieved with a near-symmetric topography and no χ differences across divides. In DAC, low-order fluvial reaches are part of the subgrid analytical topography, and they are not shown in the movie. The domain size is 50 km by 100 km, and the four edges are fixed to a constant-elevation base level. Simulation parameters are: erosivity (K) = 6.67×10^{-5} year^{-1}, x_c = 500 m, θ_c = 21°, n = 1, and m = 0.5.